Journal of Nuclear Energy Science & Power Technology

Research Article A SCITECHNOL JOURNAL

Characterization of Conical Anode: Disc Cathode Ion Source with Radial Extraction

SI Radwan[1], S Abdel Samad[2] and H El-Khabeary[1*]

[1]Accelerators & Ion Sources Department, Nuclear Research Center, P.N. 13759, Cairo, Egypt

[2]Experimental Nuclear Physics Department & Cyclotron Project, Nuclear Research Center, Cairo, Egyptian Atomic Energy Authority

***Corresponding author:** H El-Khabeary, Accelerators & Ion Sources Department, Nuclear Research Center, P.N. 13759, Egyptian Atomic Energy Authority, Cairo, Egypt, E-mail: helkhabeary@yahoo.co.uk*

Received date: February 24, 2021**, Accepted date:** March 11 2021, **Publication date:** March 18, 2021

Abstract

The main goal of this work is to study the effect of pierce angle (67.5°) of cone anode head, the exit of ion beam in a radial direction and the range of nitrogen gas operating pressure on the output ion beam current. It was found that a maximum ion beam current can be obtained in radial direction than that ion beam in axial direction which obtained in the previous study. So that a direct current conical anode-disc cathode ion source with radial extraction was designed, constructed and operated. The optimum head angle of conical anode, ion exit aperture diameter and ion exit aperture - Faraday cup distance was determined at the ion source optimum dimensions obtained previously using nitrogen gas. The electrical discharge and the output ion beam current characteristics were measured at the optimum dimensions operating conditions. It was found that at the optimum operating conditions 3 × 10^{-4} mmHg pressure, 3 kV discharge voltage and 2.2 mA discharge current, a maximum output ion beam current equal to 700 μA can be obtained. Hence, the ion source efficiency at that optimum operating conditions and discharge current equal to 0.8 mA was equal to 45%. Therefore, a comparison between the axial output ion beam current obtained in the previous study and the radial output of ion beam current measured in this study were done. Also, the effect of annealing and nitrogen ion beam irradiation on the d.c. electrical properties and micro hardness of hostaphan samples were determined.

Keywords: Radial extraction; Ion source efficiency; Nitrogen ion beam irradiation; d.c. Electrical properties; Polyethylene terephthalate

Introduction

In general, the fundamental components of ion source are the material to be ionized, the discharge chamber, material, energy source required for the ionization and the extraction system [1]. The system required to make the source operational parameters of the ion source consists of power supplies, vacuum pumping system, and measuring instrumentations. The ionization process occurs when an electron strikes the target atom or molecule, where one or more electrons are removed from the collided atom/molecule turns it into positive charge particle or increases its charge-state.

The particles with high-energy beams can be produced by using the ion sources which have many applications such as nuclear physics, isotopes separators, multi-ampere beams for fusion applications and industrial production applications [2-4]. Moreover, they can be used as tools in ion sputtering, ion implantation, ion etching, ion beam sputter deposition, neutron generators and ion beam surface modification [5-14] and. As a consequence, it is important to study the main factors which affect the characteristics of ion beams [15].

Newly, different studies based on the effect of ion beam irradiation on different polymers have an importance in the potential applications ranging from radiation dosimetry, sensors, and EMI shielding etc. [16]. The irradiation can play a vital role in enhancing the physical, structural, chemical, optical, and electrical properties of polymeric materials [17-19]. During the interaction between the polymer bonds and the ion beam, these charged particles dissipate their energy to the stopping materials mainly *via* two independent processes, *via* nuclear energy loss (ion atoms interaction) which dominates at lower energy (<1 MeV) and *via* electronic energy loss (ion electron interaction) which is prevalent at higher energies (>1 MeV) [19,20]. Furthermore, the effectiveness of changes produced in the polymers depends on the structure and parameters of the used ion beam as energy, linear energy transfer, fluence, mass, charge, beam current and also the nature of the target material itself [21-27]. The ion beam interactions with polymer result in breaking of chemical bonds, scission of the main polymer chains, cross-linking within the molecules, creation of unsaturated bonds and others [19,28].

Polyethylene Terephthalate (PET) is a polyester film with high melting point and very good mechanical properties [19]. It is used for flexible electronics [29] as well as bio-medical applications (transcatheter heart valves and artificial blood vessels) [30,31]. Also, PET based proton exchange membrane for using in fuel cells that is considered as a highly promising power source [32], also as a polymeric nuclear track detector [33], optoelectronics and in thin film processing [34,35].

The ion beams treatment allows better uniformity in the modified surface. The depth can be controlled, if its higher cross section for ionization and larger linear energy transfer [28,36]. The mechanisms of ions reacting with PET surface are very complex as the breaking chemical bond, activation, sputtering, and in most cases, combining new element onto the surface [37]. Furthermore, the kinds and working parameters of the ion beams control the content and the influence depth of new element combined onto the surface which can result in the changing of physico-chemical properties of PET surface. So, it is necessary to understand the relationship between the ion beams' working parameters and the changing of composition and properties of PET surface during the treatment process. There are various studies on the effect of nitrogen ion beam irradiation with different energies on PET that are suitable for different applications [38-41]. In this paper, the effect of ion beams exit from conical anode-disc cathode ion source with radial direction on the d.c. electrical properties and micro-hardness of PET films using nitrogen were studied.

From our previous study for the production of secondary electron emission in plasma source, it was deduced that the higher discharge current is in the case of conical anode-disc cathode ion source than the disc anode–conical cathode shapes [42]. Moreover, from another pervious study of conical anode-disc cathode ion source with axial

extraction using nitrogen gas [43]. Hence, according to these results leading us to the idea of design, construct and operate of conical anode-disc cathode ion source with radial extraction. The main idea of this paper is to study if the pierce head angle (67.5˚) of conical anode and also the exit of ion beam in radial direction (radial extraction) gives the output ion beam current compared with axial direction. In this work, we have determined the optimum head angle of conical anode, ion exit aperture diameter, $D_{ion\ exit\ aperture}$, and the distance between the ion exit aperture-Faraday cup, $d_{ion\ exit\ aperture\text{-}F.C,}$ of the conical anode-disc cathode ion source with radial extraction at the optimum dimensions of only two parameters ($d_{A\text{-}C,\ Duncovered\ A\text{-}C}$) of the conical anode-disc cathode ion source with axial extraction which obtained before using nitrogen gas [43]. The discharge and output ion beam characteristics of conical anode-disc cathode ion source with radial extraction at optimum values were measured. The ion source efficiency at the optimum dimensions using the experimental results such as electrical discharge current and the output ion beam current can be calculated. Also, the effect of nitrogen ion beam on the d.c. electrical and mechanical (micro hardness) properties of PET samples were determined and compared with the annealing effect.

Experimental Setup

Figure 1 shows a schematic drawing of copper conical anode and disc cathode ion source with radial extraction at the optimum dimensions which obtained before [43]. In which, the copper anode cone of 25.5 mm length and 30 mm diameter. The copper disc cathode has 30 mm diameter and 3.5 mm thickness. The distance between anode and cathode is equal to 32 mm. The anode and cathode are placed in a cylindrical Perspex insulator of 60 mm length, 30 mm inner diameter and 35 mm outer diameter. The inner surfaces of anode and cathode are covered with Perspex insulator disc of 30 mm diameter and 1 mm thickness except an area with diameter equal to 8 mm to confine and optimize the discharge current. The ion beam extracted from copper ion exit aperture disc of 30 mm outer diameter. Then, the output ion beam current exit through an ion exit aperture was collected and counted on Faraday cup. The nitrogen gas was admitting through a fine controlled gas admittance needle valve to control and adjust the gas flow rate.

The vacuum system consists of a high vacuum diffusion Edwards pump with speed 500 l/s to evacuate the ion source chamber in the secondary stage that accompanied by a rotary Edwards pump with speed 100 l/s to obtain a pressure until 10^{-3} mmHg in the primary stage. It is used to reach the high vacuum in the ion source chamber up to 10^{-6} mmHg for stable plasma and output ion beam. A digital compact full-range vacuum meter type 1005 Edwards was used to measure the fore and the high vacuum inside the ion source chamber.

Figure 2 shows the conical anode-disc cathode ion source with radial extraction and its associated electrical circuit. The anode, A, is connected to 5 kV-10 mA Ortec type digital Positive Power Supply (+PS) with accuracy ± 3% which used for initiating the glow discharge between the anode and cathode. A digital milli ampere meter, mA, of 0-10 mA scale range is used to measure the electrical discharge current between the anode and cathode. While a digital kilo-voltmeter, kV, of 0-5 kV scale range is used to measure the discharge voltage between them. The cathode is connected to the earth. The Faraday Cup (FC) is connected to earth through digital micro ampere meter of 0-1000 μA scale range to measure the ion beam current exit from the central aperture of the ion exit disc electrode.

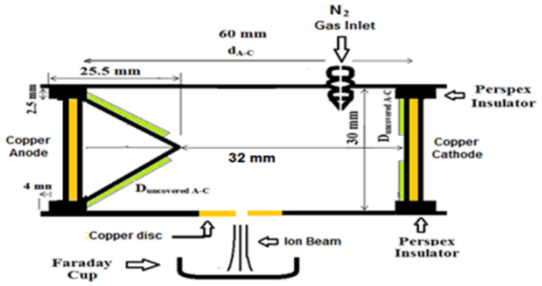

Figure 1: Conical anode-disc cathode ion source with radial extraction.

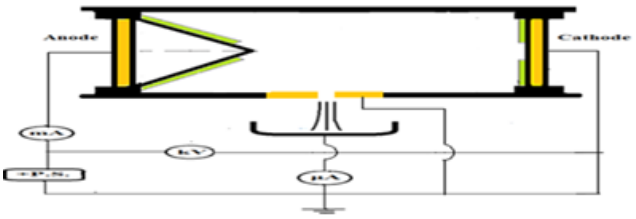

Figure 2: The electrical circuit of conical anode-disc cathode ion source.

Results and Discussions

From the previous study of conical anode-disc cathode ion source with axial extraction [43], we depend on the optimum dimensions of two parts $d_{A\text{-}C}$ and $D_{uncovered\ A\text{-}C}$. In this work, three parameters which will be optimized to reach the highest performance of the conical anode-disc cathode ion source with radial extraction that were head angle of conical anode, $D_{ion\ exit\ aperture}$, and $d_{ion\ exit\ aperture\text{-}F.C.}$ Firstly, the head angle of conical anode was varied with values equal to 30˚, 45˚, 67.5° and 75˚ to obtain the optimum angle that gave the maximum output ion beam current. Secondly, $d_{ion\ exit\ aperture\text{-}F.C}$ is fixed at 30 mm, $D_{ion\ exit\ aperture}$ was varied with values equal to 1.5, 2, 2.5, 3 and 3.5 mm and then the optimum value of $D_{ion\ exit\ aperture}$ was determined. Thirdly, $D_{ion\ exit\ aperture}$, was fixed at the optimum value, $d_{ion\ exit\ aperture\ -F.C,}$ was varied with values equal to 10, 20, 30, 40 and 50 mm and the optimum value of $d_{ion\ exit\ aperture\text{-}F.C}$ was determined. The discharge current and output ion beam current characteristics at the ion source optimum dimensions were measured at the optimum dimensions and operating conditions. Also, the ion source efficiency was determined at the optimum dimensions and operating conditions for different pressures using nitrogen gas. The comparison between the experimental results of output characteristics and their theoretical values was evaluated. Finally, the effect of annealing and nitrogen ion beam that extracted at the optimum operating conditions on the d.c. electrical and mechanical (micro hardness) properties of PET samples were determined.

Determination of optimum head angle of conical anode

In this experiment, to determine the optimum head angle of conical anode the $d_{A\text{-}C,}$ $d_{ion\ exit\ aperture\text{-}F.C.,}$ $D_{ion\ exit\ aperture,}$ and $D_{uncovered\ area\ A\text{-}C}$ were fixed at constant values equal to 32 mm, 30 mm, 2 mm, and 8 mm, respectively. Figure 3 shows the output ion beam current, I_b, versus different conical anode head angles equal to 30˚, 45˚, 67.5˚ and 75˚ of at $P=3 \times 10^{-4}$ mmHg, I_d=2.2 mA, V_d=3 kV using nitrogen gas.

It is seen that the output ion beam current is equal to 180, 360, 595 and 700 μA for head angle equal to 30˚, 45˚, 67.5˚ and 75˚respectively. It is obvious that the anode cone head angle equal to 75˚gives the highest output ion beam current.

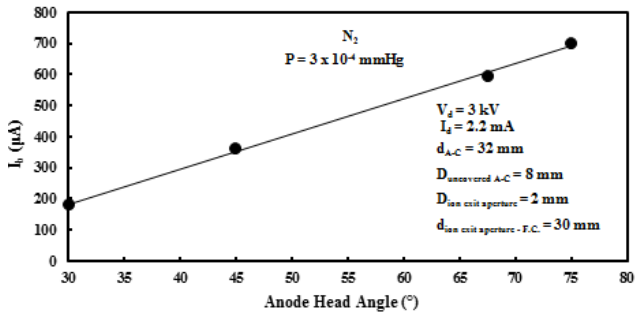

Figure 3: Output ion beam current versus different head angles of conical anode using nitrogen gas.

Determination of the ion exit aperture optimum diameter

In this experiment, the optimum head angle of conical anode equal to 75˚, $d_{ion\ exit\ aperture\text{-}F.C}$ is fixed at constant distance equal to 30 mm and $D_{ion\ exit\ aperture}$ was varied with values equal to 1.5, 2, 2.5, 3 and 3.5 mm to determine the optimum value of $D_{ion\ exit\ aperture}$. Figure 4 shows the output ion beam current, I_b (μA), versus different $D_{ion\ exit\ aperture}$ at P=3 × 10-4 mmHg, V_d=3 kV, I_d=2.2 mA, $D_{uncovered\ A\text{-}C}$=8 mm, $d_{A\text{-}C}$=32 mm, $d_{ion\ exit\ aperture\text{-}F.C.}$=30 mm and cone head angle=75º. It is obvious that at $D_{ion\ exit\ aperture}$=2 mm, a maximum output ion beam current is equal to 700 μA can be obtained. While before and after this distance, the output ion beam current decreases. This indicates that at ion exit aperture diameter equal to 2 mm and Faraday cup at a distance equal to 30 mm is that a convergent point position of ion beam which gave a maximum output ion beam current.

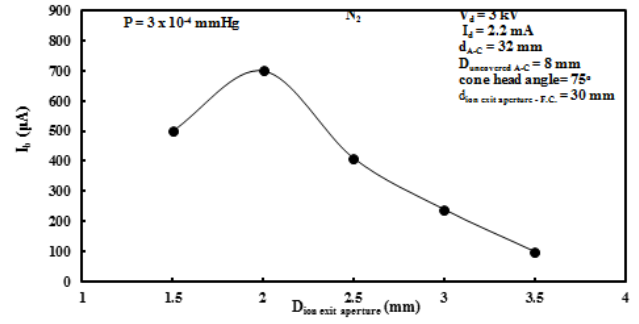

Figure 4: Output ion beam current versus different $D_{ion\ exit\ aperture}$ using nitrogen gas.

Determination of the optimum distance between ion exit aperture and faraday cup

In this experiment, the optimum head angle of conical anode equal to 75˚, Dion exit aperture is fixed at 2 mm, $d_{ion\ exit\ aperture\text{-}F.C.}$ is varied with values equal to 10, 20, 30, 40 and 50 mm and the output ion beam current was measured at each value to determine the optimum value of $d_{ion\ exit\ aperture\text{-}F.C.}$. Figure 5 shows the output ion beam current, I_b (μA), versus different $d_{ion\ exit\ aperture\text{-}F.C.}$ at P=3 × 10-4 mmHg, $D_{uncovered\ A\text{-}C}$=8 mm, $D_{ion\ exit\ aperture}$=2 mm, $d_{A\text{-}C}$=32 mm, cone head angle=75˚, Vd=3 kV and I_d=2.2 mA. It is obvious that at $d_{ion\ exit\ aperture\text{-}F.C.}$=30 mm, a maximum output ion beam current equal to 700 μA can be obtained. While before and after this distance, the output ion beam current decreases. This indicates that the extracted ion beam has a convergent point at a definite distance from the ion exit aperture of the ion source. After that point, the ion beam is divergent so the Faraday cup placed at the convergent point that gave a maximum output ion beam current.

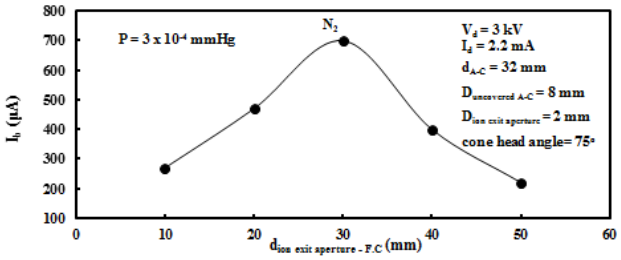

Figure 5: Output ion beam current versus different $d_{ion\ exit\ aperture\text{-}F.C.}$ using nitrogen gas.

Discharge characteristics at the optimum dimensions

Figure 6 shows the discharge current, I_d, versus discharge voltage, V_d, at different pressures and optimum dimensions that are $d_{ion\ exit\ aperture\text{-}F.C}$=30 mm, $D_{ion\ exit\ aperture}$=2 mm, $d_{A\text{-}C}$=32 mm, cone head angle=75º and $D_{uncovered\ A\text{-}C}$=8 mm using nitrogen gas. It is clear that the discharge current increases with increasing the discharge voltage. When the discharge voltage increases, the mean free path of the electrons increases and hence gain more energy to make more ionization of the gas molecules and therefore the discharge current of the formed plasma increased. For a comparison, at V_d=2.6 kV, a maximum discharge current at P=3 × 10^{-4} mmHg and 4.5 × 10^{-4} mmHg equal to 1.8 mA and 2.5 mA, respectively. This is because at the same discharge voltage, the highest gas pressure gave more ionization leading to higher discharge current than the lowest gas pressure.

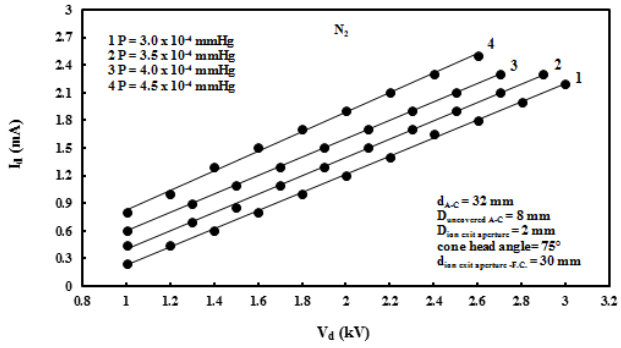

Figure 6: Discharge current versus discharge voltage at the optimum dimensions using nitrogen gas.

Figure 7 shows the output ion beam current, I_b, versus discharge current, I_d, at different pressures and optimum dimensions that are $d_{ion\ exit\ aperture\ -F.C.}$=30 mm, $D_{ion\ exit\ aperture}$=2 mm, $d_{A\text{-}C}$=32 mm, cone head angle=75º and $D_{uncovered\ A\text{-}C}$=8 mm using nitrogen gas. It was clear that the output ion beam current increases with increasing the discharge current. For a comparison, at I_d=2.2 mA, the maximum output ion beam current at P=3 × 10^{-4} mmHg and 4.5 × 10^{-4} mmHg

equal to 700 μA and 341.5 μA, respectively. At lower pressure, 3 × 10^{-4} mmHg, this allows the electrons to accept energy and hence have more mean free paths giving higher ionization of nitrogen gas molecules (high Id) than the higher pressure. So that, the ion beam extracted from the ion exit aperture without any disturbances giving more amount of output ion beam. By other words, the discharge current increases, this means that the number of ions increases and hence the output ion beam current increased.

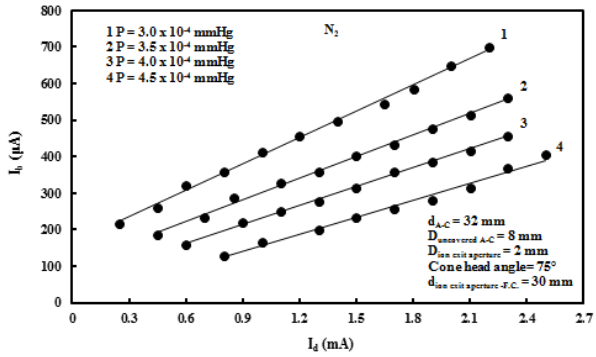

Figure 7: Output ion beam current versus discharge current at optimum dimensions using nitrogen gas.

Figure 8 shows the output ion beam current versus different pressures at different discharge voltages and optimum dimensions using nitrogen gas. It was obvious that at different constant discharge voltages, the output ion beam current decreases by increasing the gas pressure. It was found that at P=3 × 10^{-4} mmHg and discharge voltage equal to 2.6, 2 and 1 kV, the output ion beam current equal to 585, 455 and 215 μA, respectively. While at P=4.5 × 10^{-4} mmHg and discharge voltage equal to 2.6, 2 and 1 kV, the output ion beam current equal to 405, 281 and 130 μA, respectively.

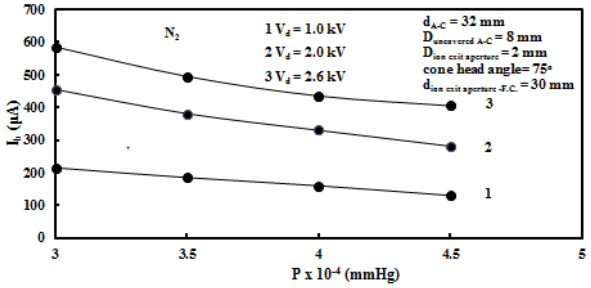

Figure 8: Output ion beam current versus different pressures at different discharge voltages and optimum dimensions using nitrogen gas.

Ion source efficiency at the optimum dimensions

The ion source efficiency at the optimum dimensions and operating parameters using the experimental results of the electrical discharge current and the output ion beam current can be calculated. Figure 9 shows the ion source efficiency, (I_b/I_d) %, versus different pressures at Id equal to 0.8, 1.2 and 2.2 mA, respectively using nitrogen gas. It is clear that at P=3 × 10^{-4} mmHg and Id equal to 0.8, 1.2 and 2.2 mA, respectively, a maximum ion source efficiency equal to 45%, 37.92% and 31.82%, respectively can be obtained. While at P=4.5 × 10^{-4} mmHg and I_d equal to 0.8, 1.2 and 2.2 mA, respectively, a maximum ion source efficiency equal to 16.25%, 15.79% and 15.45%, respectively can be obtained. This indicates that at constant ionization number, I_d, so the efficiency is increased or decreased according to the variation of the gas pressure.

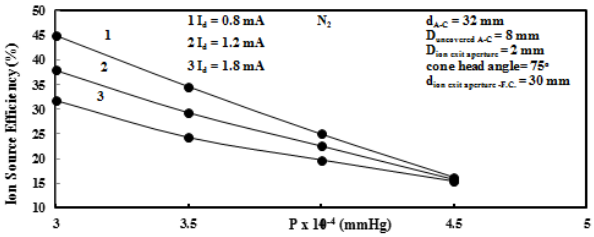

Figure 9: Ion source efficiency versus different pressures at the optimum dimensions using nitrogen gas.

Comparison between axial and radial extractions

A comparison between axial and radial extraction of output ion beam current from conical anode-disc cathode ion source was determined. Figures 10 and 11 show the discharge voltage, V_d (kV), versus discharge current, I_d (μA), and output ion beam current, I_b (μA), for conical anode-disc cathode ion source with axial extraction obtained previously [43] at optimum parameters using nitrogen gas pressures equal to 4.5 × 10^{-5} mmHg and 5.25 × 10^{-5} mmHg, respectively.

Figures 12 and 13 show the discharge voltage, V_d (kV), versus discharge current, I_d (mA), and output ion beam current, I_b (μA), for conical anode-disc cathode ion source with radial extraction at optimum parameters using nitrogen gas pressures equal to 3 × 10^{-4} mmHg and 4.5 × 10^{-4} mmHg, respectively.

It was found from these figures that the operating pressures in axial and radial extractions is different hence the discharge/output characteristics is also unlike. This is because the discharge current in case of the axial extraction in the Townsend discharge region while in case of the radial extraction in the abnormal glow discharge region.

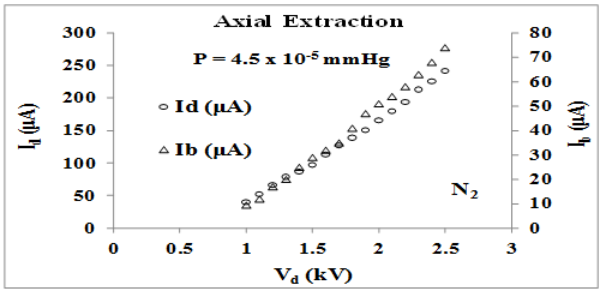

Figure 10: Discharge voltage versus discharge current and output ion beam current for conical anode-disc cathode ion source with axial extraction [43] at optimum parameters and pressure 4.5 × 10^{-5} mmHg using nitrogen gas.

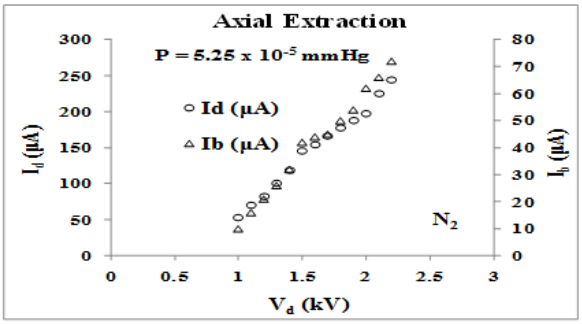

Figure 11: Discharge voltage versus discharge current and output ion beam current for conical anode-disc cathode ion source with axial extraction [43] at optimum parameters and pressure 5.25 × 10^{-5} mmHg using nitrogen gas.

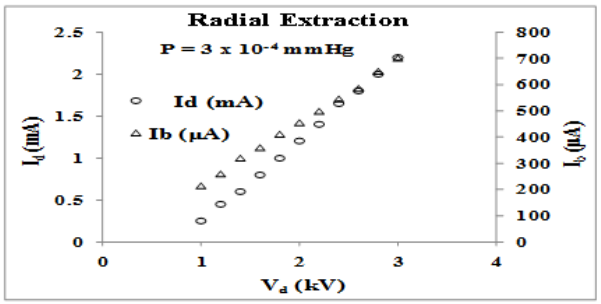

Figure 12: Discharge voltage versus discharge current and output ion beam current for conical anode-disc cathode ion source with radial extraction at optimum parameters and pressure 3 × 10^{-4} mmHg using nitrogen gas.

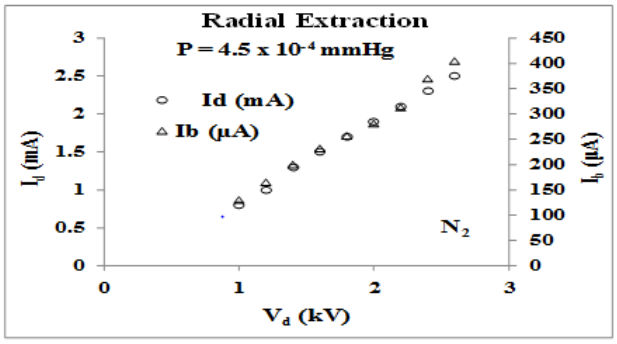

Figure 13: Discharge voltage versus discharge current and output ion beam current for conical anode-disc cathode ion source with radial extraction at optimum parameters and pressure 4.5 × 10^{-4} mmHg using nitrogen gas.

Effect of annealing and nitrogen ion beam on electrical and mechanical properties of pet samples

In this work, the d.c. electrical properties such as resistance, resistivity and conductivity were measured using Keithley electrometer model 617. Also, the mechanical properties such as micro hardness was measured using Shore D Hardness Baxlo DIN 53505 for blank and blank annealing of PET samples with thickness of 60 µm produced from Germany. D.C. electrical properties and micro hardness were studied without and with N_2 ion beam irradiation at optimum dimensions, P=3 × 10^{-4} mmHg, V_d=3 kV, I_d=2.2 mA, I_b=700 A and exposure time equal to 30 minutes. The PET sample was treated by annealing using a thermostat oven at 140°C for 30 minutes in air with heating rate equal to 5°C per 1 minute. Hence, a comparison for blank PET and blank PET annealing samples in case of without and with the irradiation of nitrogen ion beam with respect to d.c. electrical and mechanical properties were done.

Figure 14 shows the resistance values of blank and blank annealing samples without and with N_2 ion beam irradiation. It was clear that the resistance values of blank and blank annealing without N_2 ion beam irradiation were equal to 0.9181 GΩ and 0.8659 GΩ, respectively, while the resistance values of blank and blank annealing with N_2 ion beam irradiation were equal to 1.615 GΩ, 1.491 GΩ, respectively. It was clear that the resistance values of blank annealing samples without and with N_2 ion beam irradiation decreases than the resistance values of blank samples. Also, it was clear that the ion beam made cross linking in blank PET sample leading to be more resistant to the electrons movement. In addition to the annealing sample and irradiated by N_2 ion beam that the positive charges on the surface making more resistance the electrons movement.

Figure 15 shows the resistivity values of blank and blank annealing samples without and with N_2 ion beam irradiation. It was clear that the resistivity values of blank and blank annealing without N_2 ion beam irradiation were equal to 0.9181 Ω.m and 0.8659 Ω.m, respectively, while the resistivity values of blank and blank annealing with N_2 ion beam irradiation were equal to 1.615 Ω.m, 1.491 Ω.m, respectively. It was clear that the resistivity values of blank annealing samples without and with N_2 ion beam irradiation decreases than the resistivity values of blank samples. As a result of electrical resistance data, the resistivity was matching according to the direct proportional relation with resistance for the samples.

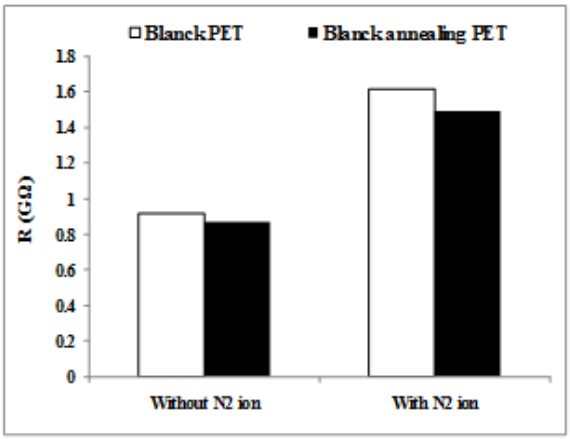

Figure 14: Resistance of blank and blank annealing blank annealing without and with N_2 ion beam using PET samples.

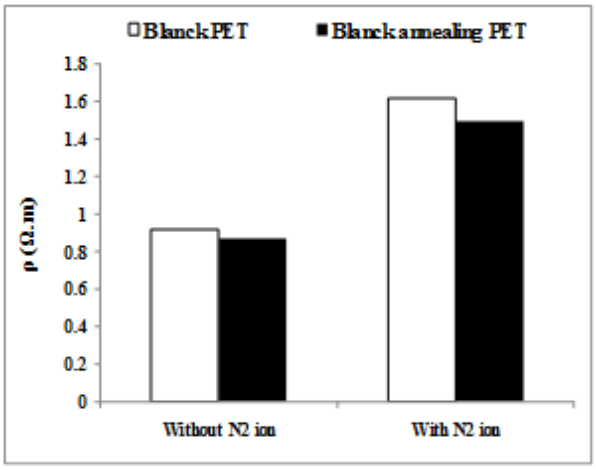

Figure 15: Resistivity of blank and without and with N_2 ion beam using PET samples.

Figure 16 shows the conductivity values of blank and blank annealing before and after N_2 ion beam irradiation using PET samples. It was obvious that the conductivity values of blank and blank annealing without N_2 ion beam irradiation were equal to 0.4818 S/m and 0.7699 S/m, respectively. It was indicated that annealing of blank PET sample has high conductivity by factor 1.6 times. While the conductivity values of blank and blank annealing with N_2 ion beam irradiation were equal to 0.4128 S/m and 0.4471 S/m, respectively. It was indicated that N_2 ion beam made the annealing blank PET sample to decrease its conductivity by factor 0.6 times compared with that in case of without N_2 ion beam and reaching nearly to the blank conductivity sample. It was clear that the conductivity values of blank annealing samples without and with N_2 ion beam irradiation increases than the conductivity values of blank samples. As we know that the electrical conductivity is directly proportional to the charge carrier density and mobility. So that the presence of positive charge (from N_2+) on the surface hindered the movement of the electrons leading to the decrease in the conductivity.

Figure 17 show the micro hardness values of blank and blank annealing samples without and with N_2 ion beam irradiation. It was obvious that the micro hardness values of blank and blank annealing without N_2 ion beam irradiation were equal to 95 Shore D and 94 Shore D, respectively. These means that the annealing effect on mechanical hostaphan has no change. While the micro hardness values of blank and blank annealing with N_2 ion beam irradiation were equal to 74.67 Shore D and 69 Shore D, respectively. It was clear that the micro hardness values of blank annealing samples without and with N_2 ion beam irradiation decreases than the micro hardness values of blank samples. Also, the ion beam effect on mechanical PET for both blank and annealing samples has a decrease change with noticeable shape. This indicates that the surface treated by ion beam becomes smoother.

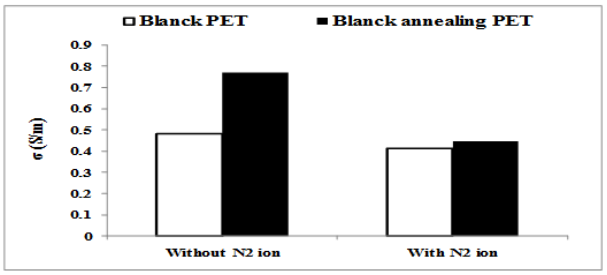

Figure 16: Conductivity of blank and blank annealing and blank without and with N_2 ion beam using PET samples.

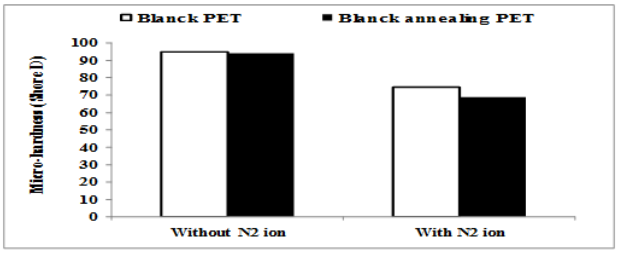

Figure 17: Micro hardness of blank annealing without and with N_2 ion beam using PET samples.

Conclusion

In this work, a direct current conical anode-disc cathode ion source with radial extraction was designed, constructed and operated. The optimum head angle of conical anode, $D_{ion\ exit\ aperture}$ and $d_{ion\ exit\ aperture\text{-}F.C.}$ were determined using nitrogen gas. The electrical discharge and the output ion beam current characteristics were measured at the optimum dimensions and operating conditions. It was concluded that at P=3 × 10^{-4} mmHg, V_d=3 kV, I_d=2.2 mA, $D_{uncovered\ A\text{-}C}$=8 mm, $d_{A\text{-}C}$=32 mm, $d_{ion\ exit\ aperture\text{-}F.C.}$=30 mm, cone anode head angle=75° and $D_{ion\ exit\ aperture}$=2 mm, a maximum nitrogen output ion beam current equal to 700 μA can be obtained. It was concluded that at the optimum dimensions and operating conditions, the efficiency of ion source with radial extraction (45%) was higher than that with axial extraction (36%). Hence, the decreased in efficiency values in case of axial extraction was due to the loss of ionization gas molecules during the collision with the cathode surface through the discharge leading to the production of secondary electrons that effected on the ion beam production. But in case of radial extraction, the ion exit aperture acts as an accelerated electrode helping the more extraction of ion beam. This was interpreted that the ion source with axial extraction operated in Townsend discharge region but the radial extraction operated at abnormal glow discharge region. Finally, it can be concluded that the nitrogen ion beam irradiation to both blank PET and annealing PET samples decreased the conductivity and micro-hardness values.

References

1. Scrivens R (2014) Classification of ion sources. 9-26.
2. Antoni V, Agostinetti P, Aprile D, Cavenago M, Chitarin G, et al. (2014) Physics design of the injector source for ITER neutral beam injector (invited). Rev Sci Instrum 85: 02B128.
3. Umeda N, Kashiwagi M, Taniguchi M, Tobari H, Watanabe K, et al. (2014) Long-pulse beam acceleration of mev-class h^- ion beams for iter n_b accelerator. Rev Sci Instrum 85: 02B304.

4. Takeiri Y, Tsumori K, Osakabe M, Ikeda K, Nagaoka K (2013) Development of intense hydrogen-negative-Ion Source for Neutral Beam Injectors at NIFS. AIP Conf Proc 1515: 139.
5. Nastasi, Mayer JW (2006) Ion implantation and synthesis of materials: pp-263.
6. Cun H, Spescha A, Schuler A, Hengsberger M, Osterwalder J, et al. (2016) Characterization of a cold cathode Penning ion source for the implantation of noble gases beneath 2D monolayers on metals: Ions and neutrals.J Vac Sci Technol A 34: 020602.
7. Helal AG, El-Khabeary H, Radwan SI (2014) Study of ion beam processing using different materials. J Nucl Ene Sci Power Generat Technol 3: 1- 8.
8. Radwan SI, Shehata MM, El-Khabeary H, Helal AG (2016) Simulation of ion beam bombardment using Bayfol CR 6-2. Radiation Physics and Chemistry 121: 93-98.
9. Behrisch R, Eckstein W (2007) Experiments and computer calculations from threshold to mev energies. sputtering by particle bombardment 110.
10. Dhayala M, Awasthic K, Vijay YK, Avasthi DK (2006) Using fast atomic source and low-energy plasma ions for polymer surface modification. Vacuum 80: 643–646.
11. Abdel Salam FW, El-Khabeary H, Abdel Reheem M (2012) Deposition of copper on glass substrate using four anode rods ion source. Arab J Nucl Sci Appl 45: 122-128.
12. Rodrguez RJ, Medrano A, Garca A, Fuentes GG, Mart´ınez R, et al. (2007) Improvement of surface mechanical properties of polymers by helium ion implantation. Surface and Coatings Technology 201: 8146-8149.
13. Helal AG, Nouh SA, El-Khabeary H (2015) Structural changes of makrofol polymer due to argon ion beam irradiation. J Nucl Ene Sci Power Generat Technol 4:1-8.
14. Valentin F, Katerina C, Thomas DG, Bruce M, Sebastian R, et al. (2017) Ion beam production and study of radioactive isotopes with the laser ion source at ISOLDE. J Phys G Nucl Part Phys 44: 084006.
15. Sadahiro T, Matsuyama K, Kiuchi M, Matumoto T, Takizawa T et al. (2004) Improvement in ion beam quality for thin-film formation. Surface and Coatings Technology 188: 265-267.
16. El-Badry BA, Zaki MF, Hegazy MT, Morsy (2008) An optical method for fast neutron dosimetry using CR-39. Radiat Eff Defects Solids 163: 821-825.
17. Shehata MM, SI Radwan, Saleh HH, Ali ZI (2020) γ-Rays and ion beam irradiation effects on the optical and structural properties of poly (vinyl alcohol)-ethylene glycol composite. J Radioanal Nucl Chem 323: 897-902.
18. Radwan SI, Abdel Samad S, El-Khabeary H (2020) Influence of temperature and frequency on electrical properties of gold/ PM-355 thin films treated by annealing and nitrogen ion beam. Indian J Phys.
19. Radwan SI, Rashad AM, Tantawy HR (2020) 10th International Conference on Engineering Mathematics and Physics (ICMEP-10). Military Technical College 7-9.
20. Behar M (2004) Fundamentals of Ion-irradiated Polymers 63: 406.
21. Marletta G (1990) Chemical reactions and physical property modifications induced by kev ion beams in polymers. Nucl Instrum Methods Phys Res B 46: 295–305.
22. Calcagno L, Compagnini G Foti G (1992) Structural modification of polymer films by ion irradiation. Nucl Instrum Methods Phys Res B 65: 413–422.
23. Arif S, Saleemi F, Shahid Rafique M, Naab F, Toader O, et al. (2016) Effect of silver ion-induced disorder on morphological, chemical and optical properties of poly (methyl methacrylate). Nucl Instrum Methods Phys Res B 387: 86–95.
24. Fink D (2004) Ion-Beam radiochemistry. Fundamentals of Ion Irradiated Polymers 63: 251-307.
25. Billmeyer FW, John W Sons (1984) Text book of polymer science (third edition). J Polym Sci Polym Lett Ed 22: 596.
26. Chawla M, Aggarwal S, Sharma A (2017) Rutherford backscattering spectrometry studies of 100 kev nitrogen ion implanted polypropylene polymer. Nucl Instrum Methods Phys Res B 407: 125–131.
27. GoyaL PK, Kumar V, R. Gupta, Mahendia S, Anita et al. (2011) Study of electrical and structural modifications induced by 100 kev argon ions in poly(ethylene terephthalate). Adv Appl Sci Res 2: 77–82.
28. Popok VN (2012) Ion implantation of polymers: formation of nanoparticulate materials. Rev Adv Mater Sci 30: 1–26.
29. Zardetto V, Brown TM, Reale A, Di. Carlo A (2011) Substrates for flexible electronics: A practical investigation on the electrical, Film Flexibility, Optical, Temparature and Solvent Resistance Properties. J Polym Sci B Polym Phys 49: 638-648.
30. Karck M, Forgione L, Haverich A (1993) The efficacy of controlled antibiotic release for prevention of polyethyleneterephthalate-(Dacron-) related infection in cardiovascular surger. Clin Mater 13: 149-154.
31. Struszczyk MH, Bednarek P, Raczynski K, Polim (2002) Synthetic vascular prostheses. Med 32: 13-22.
32. Abdel-Hady EE, Abdel-Hamed AA, Gomaa MM (2013) Preparation and characterization of commercial polyethyleneterephthalate membrane for fuel cell applications. J Membra Sci Technol 3: 8.
33. Kusumoto T, Barillon R, Yamauchi T (2019) Applications of radial electron fluence around ion tracks for the description of track response data of polyethylene terephthalate as a polymeric nuclear track detector. Nucl Instrum Methods Phys Res B 461: 260-266
34. Liu Q, Yang X, Chen X, Mingwang M, Kang Y, et al. (2009) Influence of pore size and pore shape on thermo-sensitive properties of poly ((ethylene terephthalate)-graft-(n-isopropylacrylamide)) track membranes. Polym Int 58: 1078–1083.
35. Ryu G, Jeong SH, Park BC, Beob P, Chung K (2014) Fabrication of organic thin film transistors on Polyethylene Terephthalate (PET) fabric substrates. Org Electron 15: 1672–1677.
36. Drabik M, Dworecki K, Tańczyk R, Wąsik S, Żuk J (2007) Surface modification of PET membrane by ion implantation. Vacuum 81: 1348.
37. Dinga W, Jud D, Chai W (2010) The effect of working pressure on the chemical bond structure and hydrophobic properties of PET surface treated by N ion beams bombardment. Appl Surf Sci 256: 6876–6880.
38. Nathawat R, Kumar A, Kulshrestha V (2008) Study of surface activation of PET by low energy (keV) Ni^+ and N^+ ion implantation. Nucl Instrum Methods Phys Res Sect B 266: 4749-4756.

39. Dworecki K, Hasegawa T, Sudlitz K, Wąsik S (2000) Modification of electrical properties of polymer membranes by ion implantation. Nucl Instrum Methods Phys Res B: Beam Interact Mater Atoms 166: 646-649.
40. Maletic SB, Cerovic, Dojcilovic JR (2019) A study of structural and spectral properties of ion-beam modified polyethylene terephthalate membrane. Nuclear Instrum Methods Phys Res Sect B 441: 1-7.
41. Sharma T, Agrawal S, Sharma A, Kumar S, Kanjilal D, Deshpande SK and Goyal PS (2007) Modification of optical properties of polycarbonate by gamma irradiation. J Appl Phys 102: 063527.
42. Radwan SI, El-Khabeary H, Helal AG (2017) Verification of paschen law using a mixed geometry discconical electrodes.
43. Abdel Samad S, Radwan SI, El-Khabeary H (2018) Investigation of conical anode–disc cathode ion source. Can J Phys 96: 194-201.